Nuclear Instruments and Methods in Physics Research A 645 (2011) 266–272

Contents lists available at ScienceDirect

Nuclear Instruments and Methods in Physics Research A

journal homepage: www.elsevier.com/locate/nima

Numerical simulation methods for electron and ion optics

Eric Munro

Munro's Electron Beam Software Ltd., 14 Cornwall Gardens, London SW7 4AN, England

ARTICLE INFO

Available online 22 December 2010

Keywords:
CAD software
Field computation
Ray tracing
Electron optics
Simulation methods
Aberrations

ABSTRACT

This paper summarizes currently used techniques for simulation and computer-aided design in electron and ion beam optics. Topics covered include: field computation, methods for computing optical properties (including Paraxial Rays and Aberration Integrals, Differential Algebra and Direct Ray Tracing), simulation of Coulomb interactions, space charge effects in electron and ion sources, tolerancing, wave optical simulations and optimization. Simulation examples are presented for multipole aberration correctors, Wien filter monochromators, imaging energy filters, magnetic prisms, general curved axis systems and electron mirrors.

1. Introduction

For design and optimization of electron and ion beam equipment, numerical simulation methods are indispensible. When digital computers first became widely available, in the 1950s and 1960s, methods were developed for computing fields, trajectories and aberrations in electron lenses, and such simulations played a key role in improving the design of electron microscopes. Since then, the electron and ion beam equipments themselves, and the computer simulation methods used in their design, have progressed almost beyond recognition.

This paper surveys simulation techniques, and illustrates the complexity of equipment designs to which they can be applied. Topics covered include computation of fields (Section 2), optical properties (Section 3), Coulomb interactions (Section 4), space charge effects in electron and ion sources (Section 5), tolerancing (Section 6), wave optics (Section 7) and optimization (Section 8). Several illustrative examples are presented (Section 9), including multipole aberration correctors, monochromators, imaging energy filters, magnetic prisms, curved axis systems and electron mirrors.

2. Field computation

The three main techniques for computing electric and magnetic fields are Finite Difference Method ("**FDM**"), Finite Element Method ("**FEM**") and Boundary Element Method ("**BEM**"). These are widely described in the literature, so are just summarized briefly here.

In **FDM** [1], the space enclosing the electrodes or polepieces is covered with a mesh, and Laplace's equation is approximated at each mesh point by a "Finite Difference Equation", which expresses the potential at the central point as a weighted sum of the potentials at n surrounding points (usually $n=4$ for planar or rotational symmetry, or $n=6$ for 3D simulations). The resulting equations are solved by "Successive Over-Relaxation" ("SOR") [2] or "Multi-Grid" ("MG") [3] methods, to obtain the potential distribution.

In **FEM** [4,5], a deformable mesh is used, chosen to fit the electrode or polepiece geometry (Fig. 1). The quadrilateral areas of the mesh are called "Finite Elements". Using bi-linear interpolation of the potential in each element, the field energy stored in each finite element is expressed in terms of the potentials at the element's 4 nodes (Fig. 2a). The requirement that the total field energy be minimized is used to derive a set of "Finite Element Equations", relating the potential at each mesh point to the potentials at the 8 surrounding points. The resulting 9-point Finite Element Equations are solved by the ICCG method [6], to obtain the potential distribution. It is also possible to use Finite Elements with 9 nodes, called "Second Order Finite Elements" ("SOFEM") (Fig. 2b), with bi-quadratic potential variation, and the elements can have curved edges. The principle is the same as for first order FEM ("FOFEM"), but in SOFEM [7] 25-point FE equations are obtained. The bi-quadratic potential in SOFEM has less truncation error than FOFEM, so is intrinsically more accurate for a given number of mesh points. The curved elements in SOFEM are also useful for fitting curved electrodes (e.g. spherical cathodes). Advantages of FEM include the ease with which it handles dielectrics, ferromagnetic materials, magnetic saturation and permanent magnets.

In **BEM** [8], the electrode surfaces are discretized into N small surface elements called "Boundary Elements" (Fig. 3). A surface charge density σ_i is assigned to the ith Boundary Element, and an integral equation is used to express the potential Φ_j on the jth Boundary Element as a weighted sum of the surface charge densities σ_i on all N Boundary Elements. As the electrode potentials

E-mail address: eric@mebs.co.uk

0168-9002/$ - see front matter © 2011 Elsevier B.V. All rights reserved.
doi:10.1016/j.nima.2010.11.181

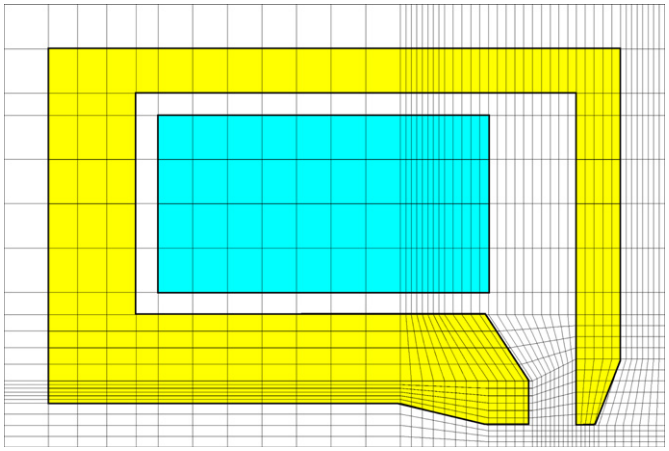

Fig. 1. Example of finite element mesh layout for a magnetic lens. The quadrilateral finite elements are arranged to fit the magnetic circuit and coil winding geometry.

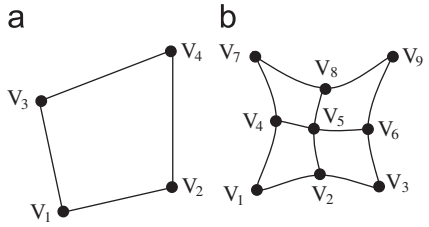

Fig. 2. Finite Elements. (a) First order—with 4 nodes, straight edges and bi-linear potential variation. (b) Second order—with 9 nodes, curved edges and bi-quadratic potential variation.

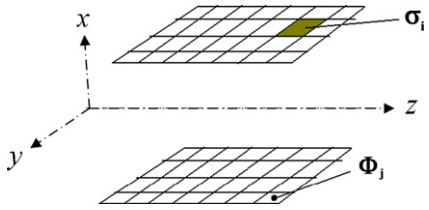

Fig. 3. Boundary Element Method. Electrode surfaces are discretized into small Boundary Elements with surface charge densities σ_i ($i=1, \ldots, N$), which are computed to satisfy the known boundary potentials Φ_j ($j=1, \ldots, N$).

Φ_j are known *a priori*, this yields a set of N simultaneous equations that can be solved for the surface charge densities σ_i. The potential Φ at any point can then be computed with an integral equation over the surface charge densities σ_i.

After computing the potential distribution with FDM, FEM or BEM, the potential or field along the axis is usually required for computing the optical properties. For electrostatic lenses, the axial potential is obtained directly from the axial mesh points. For other electron optical components, axial field functions (e.g. axial flux density $B(z)$ for a magnetic lens) are obtained by numerical differentiation of the mesh-point potentials, e.g. using spline curves.

3. Optical properties

We summarize here three methods for computing optical properties: (i) Paraxial Rays and Aberration Integrals, (ii) Differential Algebraic Method and (iii) Direct Ray Tracing.

Paraxial Rays and Aberration Integrals: Paraxial Rays are computed by solving a "Paraxial Ray Equation" and aberration coefficients using "Aberration Integrals", starting from the computed axial field functions. Paraxial ray equations can be solved by Runge–Kutta method and Aberration Integrals can be evaluated with Simpson's rule. This method is easy to program and fast to run for electron lenses and deflectors. Its main limitations are: (i) a separate integral is required for each aberration coefficient (although using Paraxial Rays as dummy arguments helps); (ii) components with different symmetries (e.g. round lenses, deflectors, multipole lenses) require individual formulae; (iii) higher order Aberration Integrals are complicated (although algebraic manipulation languages, like CAMAL [9] or MOPS [10], can help) and (iv) aberration formulae for electron mirrors are very complicated [11].

Differential Algebraic ("DA") Method: This method [12] overcomes the above limitations. "Differential Algebraic" Quantities ${}_nD_\nu$ are defined, which are polynomials of order n in ν variables. A "Differential Algebra" is defined for operations on these quantities, such as. +, −, ×, /, √, etc. These DA Quantities and Operators are programmed as a C++ Class to form a new data type. The ray coordinates $x(z)$, $y(z)$ are now expressed as functions of z along the optical axis, in powers of the initial position (x_o, y_o), initial slope (x'_o, y'_o) and initial energy deviation (ΔV) at object plane z_o. The 5 quantities $(x_o, y_o, x'_o, y'_o, \Delta V)$ are our expansion variables for the aberrations, so we use DA Quantities with $\nu=5$ variables. The order n used for the DA Quantities is the maximum rank to which we want to compute the aberrations. We replace the real coordinates and slopes (x, y, x', y') in the equations of motion by their DA Quantities (X, Y, X', Y') and then solve the equations of motion numerically, e.g. using a Runge–Kutta formula, in a single DA Ray Trace from object plane z_o to image plane z_i. The DA Ray Trace maps the system aberrations, up to rank n, as functions of z. The first order terms in the DA Quantities contain the paraxial rays, and the ith order terms contain the ith rank aberrations.

For applying the DA method, the axial field functions must be differentiable to n-th order. We achieve this in our software by fitting the axial fields with Hermite functions [13].

The DA method requires only a single Ray Trace, no Aberration Integrals, and handles any type of symmetry. It can compute aberrations of electron mirrors, by writing the equations of motion with time t as independent variable [14]. Relativistically correct aberrations up to n-th rank can be obtained, simply using the relativistically correct equations of motion.

Direct Ray Tracing: This involves solving the Newton–Lorentz equation of motion

$$\frac{d}{dt}(m\mathbf{v}) = q(\mathbf{E}+\mathbf{v}\times\mathbf{B})$$

directly, where m=particle mass, q=charge, $\mathbf{v}$=velocity, $\mathbf{E}$=electric field, $\mathbf{B}$=magnetic flux density. In our implementation, the $\mathbf{E}$ and $\mathbf{B}$ fields at any point are obtained by fitting the numerical axial field functions with Hermite functions and using power series expansions for the field components at off-axis points. Trajectories are computed from z_o to z_i with any given initial position and slope, and aberration diagrams can be plotted directly (Fig. 4). By choosing rays with suitable initial conditions at z_o, and solving a few simultaneous equations, the aberrations at the image plane z_i can be extracted from the direct ray trace.

4. Discrete Coulomb interactions

In electron and ion beams, there are Coulomb forces between every pair of particles. The axial components of these forces increase the energy spread ("Boersch effect") [15], and the transverse components cause radial broadening ("Loeffler effect") [16]. These effects increase with beam current and limit the throughput in charged particle lithography [17].